Polymer Journal, Vol. 19, No. 3, pp 315—322 (1987)

Structural Factor Governing Dyeability of Poly(ethylene terephthalate) Fibers

Kenji KAMIDE and Tomio KURIKI

Fundamental Research Laboratory of Fibers and Fiber-Forming Polymers, Asahi Chemical Industry Co., Ltd., 11-7 Hacchonawate, Takatsuki, Osaka 569, Japan

(Received May 16, 1986)

ABSTRACT: An attempt was made to clarify whether there is a structural factor governing the dyeability of poly(ethylene terephthalate) (PET) fibers by disperse dye or not, and if so what it is. Five PET fiber samples having a wide degree of amorphous packing (n) distribution, $F'(n)$, as determined from dynamic loss tangent–temperature curves in an α_a dispersion region using Manabe and Kamide's method, were prepared by changing spinning velocities and annealing conditions. PET fibers were dyed with the three different disperse dyes under various conditions and the dye uptake W was determined colorimetrically. The upper limit of n, denoted as n_u°, above which the dye molecule can not penetrate through amorphous regions, was evaluated as functions of dyeing conditions from the plots of W against $G(n_u)$ ($\equiv \int_{-\infty}^{n_u} F'(n)dn$) obtained for various assumed n_u. It was confirmed that the plots of W *vs.* $G(n_u^\circ)$ give a single master line, irrespective of the various fiber preparing conditions or dyeing conditions; for Resolin Blue FBL $W = 67.6 \cdot G(n_u^\circ) - 0.4$ (mg-dye/g-fiber). This indicates that the dyeability of PET fibers by the disperse dye is unambiguously governed by the amount of the amorphous region, whose degree of amorphous packing of n is not larger than n_u°.

KEY WORDS Dyeability / Disperse Dye / Structural Factor / Dye Uptake / Degree of Amorphous Packing Distribution / Viscoelastic Property / Poly(ethylene terephthalate) /

The structural factors controlling the dyeability of PET fibers by the disperse dyes have not yet been systematically studied: Kitamura *et al.*[1] found that (1) the penetration coefficient of a dye in heat-treated PET fibers increased with the intensity of the X-ray small-angle scattering and the gauche content of the ethylene glycol unit in the amorphous region, and (2) with an increase in the temperature or time of heat-treatment, the X-ray intensity increased and the gauche content decreased. Yonetake *et al.*[2] applied the mosaic block model for the dyeability of heat-treated polypropylene films, and found that the crystallinity and the crystalline size especially in the direction of chain axis, as determined by the X-ray diffraction method, increased with heat-treatment and concluded that dye molecules were adsorbed more in the amorphous side region located between cores parallel to the chain axis than in the amorphous end region between lamella surfaces. However, note that these studies lack in the direct evaluation of the fine structure.

In the previous note,[3] we demonstrated that the dyeability of poly(ethylene terephthalate) (PET) fibers by a disperse dye at 100—130 °C has a close relationship against the maximum value of the mechanical loss tangent, $(\tan\delta)_{max}$, in their microbrownian movement (α_a) regions and the temperature T_{max}, at which $(\tan\delta)_{max}$ is attained. Both parameters can be experimentally determined with good accuracy from the dynamic viscoelasticity *vs.* temperature (T) curve in the α_a dispersion region. Recently, Manabe and

Kamide defined the second order structure characterized by the aggregation state of a polymer chain in a hypothetical cubic body with one side about 10 nm in length.[4] They also introduced the degree of amorphous packing, n, of polymer segments for the second-order element, whose peak temperature of $\tan\delta$ is T'_{max}, by

$$n=(T'_{max}-T_{max})/(\Delta T_{1/2})_R \quad (1)$$

where $(\Delta T_{1/2})_R$ is the half-value width of the $\tan\delta$–T curve of the second-order element. They showed theoretically that the distribution function $F'(n)$ of the degree of amorphous packing, n, can be directly estimated from $\tan\delta$–T curve in the α_a dispersion. Completely amorphous polymers, including atactic polystyrene, have very narrow n distributions, but semicrystalline polymers generally show significantly broad n distributions. PET fibers obviously belong to the latter category. Alternatively, n is also defined by the equation 1′

$$n=\frac{\bar{f}-f}{\Delta\alpha(\Delta T_{1/2})_R} \quad (1)'$$

where f is the free volume fraction, $\bar{f}$, f at $n=0$, and $\Delta\alpha$ is the difference in the volume expansion coefficients above and below T_g. Therefore, the dye molecule expected to penetrate preferentially into the region with lower degree of amorphous packing by the segmental motions of amorphous chains and in consequence, the dyeability should be governed by $F'(n)$. This article confirms the above expectation by experimental results.

THEORETICAL BACKGROUND

According to Manabe and Kamide's theory,[4,5] the region having the degree of amorphous packing of n lower than a specific value n_u, $G(n_u)$, is given by

$$G(n_u)=\int_{-\infty}^{n_u} F'(n)\,dn \quad (2)$$

where $F'(n)$ is normalized for a unit mass of the polymer sample.

If we suppose that the dye molecule can diffuse only into the region related to $G(n_u^\circ)$ having n not larger than n_u°, the dye uptake W should be linearly proportional to $G(n_u^\circ)$:

$$W=k\cdot G(n_u^\circ) \quad (3)$$

where k is a proportional constant.

If the dye uptake for unit mass of a polymer sample possibly changes with n, then k should be expressed as a function of n, $k(n)$, and eq 3 can be generalized in the form,

$$W=\int_{-\infty}^{n_u^\circ} k(n)\cdot F'(n)\,dn \quad (4)$$

Analysis of the experimental data according to eq 4 is very difficult without detailed knowledge on $k(n)$.

Under the following conditions

$$k(n)=k,\ n\leqq n_u^\circ$$
$$k(n)=0,\ n>n_u^\circ \quad (5)$$

eq 4 reduces readily to eq 3 and n_u° can be determined in the manner that W is proportional to $G(n_u^\circ)$. n_u° varies with dyeing temperature T_d, dyeing time t_d and the molecular structure of the dye employed and is independent of $F'(n)$. This procedure was successfully applied in part by Nakayama *et al.*[6] in their study on the dyeing of polyacrylonitrile fibers. When eq 3 is acceptable, a master curve should be obtained between W and $G(n_u^\circ)$ for various fiber samples, dyed under different conditions.

EXPERIMENTAL

Five PET filaments (75 denier/36 filaments), melt spun from PET chips of the viscosity-average molecular weight $\bar{M}_v=4.4\times10^4$ at various spinning velocities ranging 1.5—8.0×10^3 m min^{-1}, were utilized. The preparing conditions of these samples are summarized in Table I. The detailed prepar-

Table I. Conditions for the preparation of poly(ethylene terephthalate) filaments (viscosity-average molecular weight $\bar{M}_v = 4.4 \times 10^4$, 75 denier/36 filaments) with different amorphous structures

Sample code	Spinning process velocity/m min^{-1}	Annealing process		Drawing process	
		Temperature, T_a/°C	Time, t_a/s	Draw ratio	Temperature/°C
PD-1	4000	250	1	—	—
PD-2	8000	250	1	—	—
PD-3	7000	170	1	—	—
PD-4	5000	170	1	—	—
PD-5	1500	—	—	3.9	130

ing procedure has already been described elsewhere.[7] The as-spun filaments were heat-treated at 170 or 250°C for 1 s, using a special annealing apparatus, designed and constructed before,[7] or drawn at 130°C to give five samples differing greatly in $F'(n)$.

For the samples tan δ–T curves were determined using a Rheovibron DDV-IIc at 110 Hz and at a heating rate of 10 K min^{-1}. By examination of the curve obtained using Manabe and Kamide's method,[4] $F'(n)$ was evaluated.

Three disperse dyes were utilized: Resolin Blue FBL (RBF) (1,8-dihydroxy-2-bromo-4,11-diamino-anthraquinone, molecular weight = 349, manufactured by Bayer AG (Leverkusen DBR)), Diacelliton Fast Orange GL (DFO) (4-nitro-4′-amino-azobenzene, molecular weight = 242, manufactured by Mitsubishi Chemical Co., Ltd.), and Miketon Fast Red R (MFR) (4-nitro-4′(*N*,*N*-dihydroxyethyl)-amino-azobenzene, molecular weight = 344, manufactured by Mitsui-Toatsu Chemical Co., Ltd.). These dyes were purified by recrystallization from their acetone solutions. The molecular structures of the dyes are shown in Figure 1. DFO and MFR are similar in chemical structure and differences in dyeability, if any, may be due to molecular weight difference. RBF and MFR have almost the same molecular weight, but differ in molecular shape. The PET samples were dyed under the following conditions: dye concentration, 1.2 g l^{-1}; liquor ratio, 200; dyeing temperature (T_d), 90, 100, 110, and 130°C; dyeing time (t_d), 30—360 min.

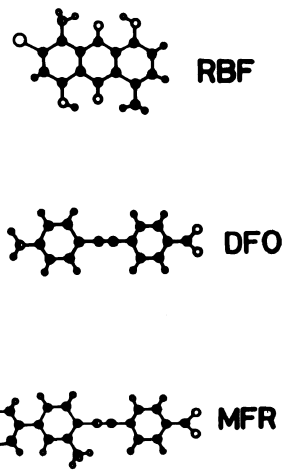

Figure 1. Chemical structures of three dyes utilized in this study: RBF, Resolin Blue FBL; DFO, Diacelliton Fast Orange GL; MFR, Miketon Fast Red R. Filled circle, carbon atom; small unfilled circle, hydrogen atom; middle unfilled circle, oxygen atom; half-filled circle, nitrogen atom; large unfilled circle, bromine atom.

The dyed sample (0.1 g) was twice washed with distilled water at room temperature and then extracted with a 100 ml of *N*,*N*-dimethylformamide (DMF) at 60°C. The extraction procedure was repeated three times and the extracts were gathered and diluted with fresh DMF to give a 500 ml solution. The total amount of dye absorbed by a fiber was colorimetrically determined on a Shimadzu UV-360 type spectrophotometer.

RESULTS AND DISCUSSION

Figure 2 shows the $F'(n)$ curve of PET fibers prepared in this study. Here, the T_{max} ($=128°C$) of the sample code PD-5 was decided at $n=0$. The five samples have widely different $F'(n)$: for example, sample code PD-2 and PD-3 contain larger amounts of low n region than sample code PD-4. It has already been confirmed that $F'(n)$ of the samples does not change during the dyeing process.

Figure 3 shows that dye uptake W depends on t_d. In the range of $t_d < 360$ min, W does not reach its asymptotic value; at $T_d \geqq 130°C$, the order of the magnitude of W in five samples changes sometimes with t_d.

Figure 4 shows some examples of the relations between W and $G(n_u)$. The number in the figure is the assumed value of n_u. For a specific n_u (n_u°), W is proportional to $G(n_u)$. When the linear relationship between W and $G(n_u^\circ)$ holds, the W value of intercept at $G(n_u^\circ)=0$ should be zero. This intercept value of W is given by the product of the slope, $\tan\alpha$, of the plot in Figure 4 and absolute value of an intercept at $W=0$, $|\lim_{W\to 0} G(n_u^\circ)|$. Then the product of $\tan\alpha \cdot |\lim_{W\to 0} G(n_u^\circ)|$ can be employed as a measure of the deviation of the W *vs.* $G(n_u^\circ)$ plots from eq 3.

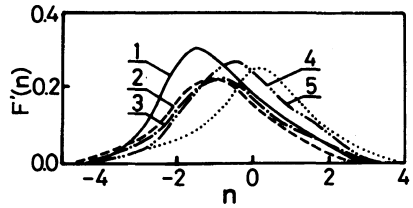

Figure 2. Normalized degree of amorphous packing distribution $F'(n)$ of the amorphous region of PET fibers: 1, sample code PD-1; 2, sample code PD-2; 3, sample code PD-3; 4, sample code PD-4; 5, sample code PD-5; see also Table I.

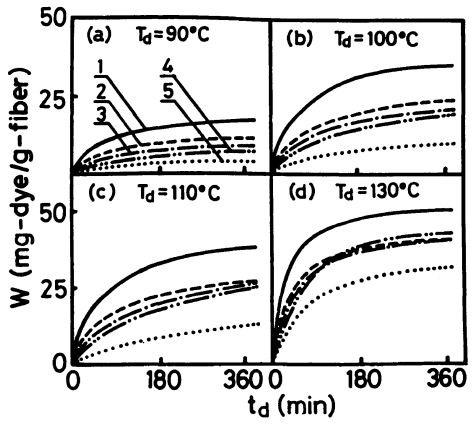

Figure 3. Change in the dye uptake W of RBF with the dyeing temperature T_d and the dyeing time t_d. Numbers on curves have the same meaning as those in Figure 2.

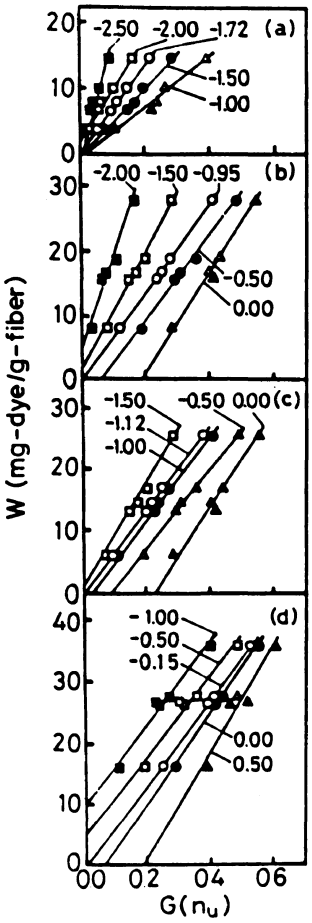

Figure 4. Plot of the dye uptake W of RBF *vs.* $G(n_u)$. a) $T_d=90°C$, $t_d=360$ min; b) $T_d=100°C$, $t_d=360$ min; c) $T_d=110°C$, $t_d=240$ min; d) $T_d=130°C$, $t_d=120$ min. Numbers on the curves mean the assumed n_u values.

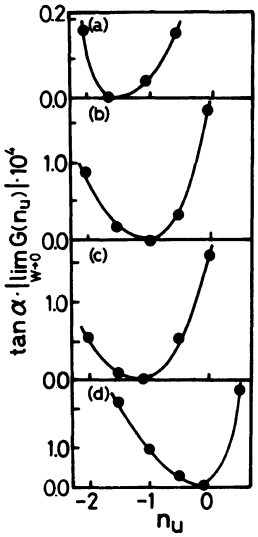

Figure 5. The production of $\tan\alpha \cdot |\lim_{W\to 0} G(n_u)| \times 10^4$ plotted as a function of the assumed n_u for RBF. a) $T_d = 90°C$, $t_d = 360$ min; b) $T_d = 100°C$, $t_d = 360$ min; c) $T_d = 110°C$, $t_d = 240$ min; d) $T_d = 130°C$, $t_d = 120$ min.

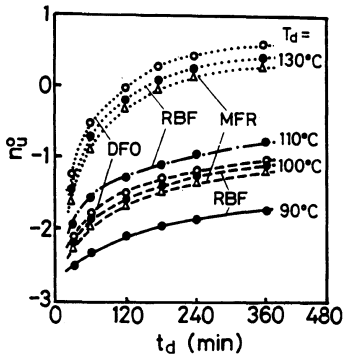

Figure 6. Change in n_u° with dyeing time t_d: full line, $T_d = 90°C$; broken line, $T_d = 100°C$; chain line, $T_d = 110°C$; dotted line, $T_d = 130°C$; ○, DFO; ●, RBF; △, MFR.

Figure 5 shows the plot of $\tan\alpha \cdot |\lim_{W\to 0} G(n_u^\circ)|$ *vs.* n_u constructed from the data in Figure 4. The n_u value corresponding to the minimum of the product is the true n_u°. The n_u° values for other dyeing conditions, not shown in Figures 3 and 4, was also determined using the present method.

Figure 6 shows the effects of the dyeing conditions (T_d and t_d) on n_u°. The dye molecule with larger molecular weight penetrates into the larger n region as the sample is dyed at higher temperature for a longer period. The t_d dependence of n_u in shorter t_d becomes remarkable at higher T_d.

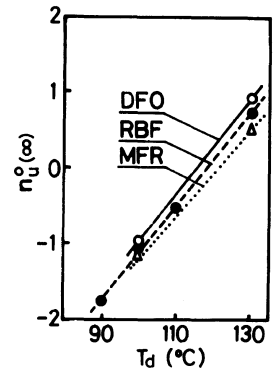

Figure 7. Relations between $n_u^\circ(\infty)$ and dyeing temperature T_d.

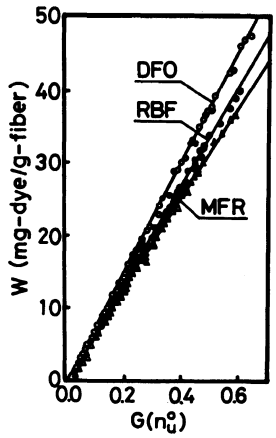

Figure 8. Experimental relations between the dye uptake W and $G(n_u^\circ)$ for PET fibers.

We estimated n_u° at infinite time of t_d, $n_u^\circ(\infty)$, by extrapolating the curves in Figure 6 to the infinite value of t_d and plotted it as a function of T_d in Figure 7. The $n_u^\circ(\infty)$ value increases linearly with T_d. At higher T_d, the dye can penetrate into a more closely packed region of the amorphous phase. $n_u^\circ(\infty)$ decreases in the following order at a given T_d: DFO > RBF > MFR.

Figure 8 summarizes the relations between

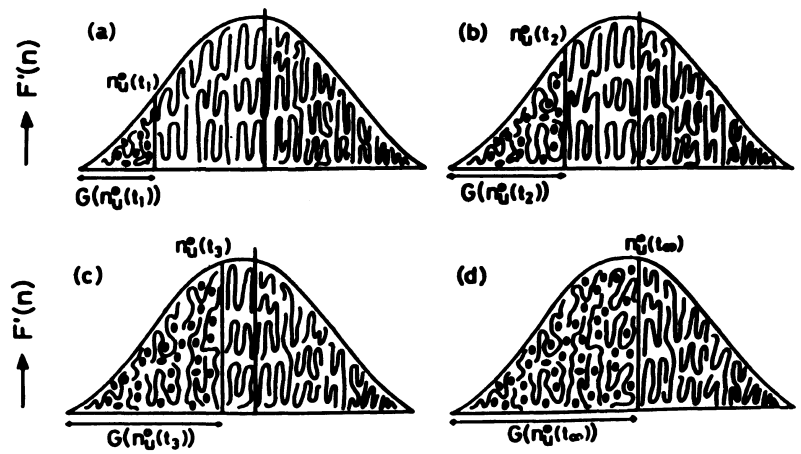

Figure 9. Schematic representation of the dyeing phenomena of amorphous region, represented by $F'(n)$, as a function of dyeing time t_d. Black circles indicate dye molecules.

W and $G(n_u^\circ)$, obtained for various samples dyed under various conditions. All the experimental points for each dye fall on a single straight master line expressed by

$$W = 67.6 \cdot G(n_u^\circ) - 0.4 \quad \text{for RBF} \quad (6a)$$

$$W = 75.3 \cdot G(n_u^\circ) - 0.4 \quad \text{for DFO} \quad (6b)$$

$$W = 63.0 \cdot G(n_u^\circ) - 0.3 \quad \text{for MFR} \quad (6c)$$

using the least-squares method. The second term of the right-hand side in eq 6 can be neglected with good approximation as compared with the first term of the same side; then eq 6 can be regarded as an experimental expression for eq 3. Figure 6 indicates that k in eq 3 is constant for a given dye, irrespective of various PET samples and the dyeing conditions. Different k values were obtained for different dye molecules.

As long as disperse dyes are utilized, the dyeability of PET fibers is unambiguously determined by the amount of amorphous region, where the degree of amorphous packing n is not larger than n_u°.

The slope of the plots in Figure 8 is not a single function of the molecular weight of the dye, but depends on the general shape of the dye molecule and probably on the PET molecule–dye molecule interaction. For example, RBF and MFR have similar molecular weight (345 ± 5). Note that the axial ratio of the RBF molecule is not far from unity, but that of MFR is larger than 3. It is clear that the PET (and probably any) fibers can be dyed easily with dyes of smaller molecular weights and compact form.

On the basis of the experimental results obtained here, we can speculate the detailed mechanism of dyeing of PET fibers with disperse dye. Figure 9 shows a schematic representation of the dyeing phenomena of the amorphous region as a function of dyeing time t_d. In the figure, the black circle is the dye molecule. Explanations for Figure 9 are given as follows.

(1) At given T_d, the PET molecules in the amorphous region not larger than n_u° have vigorous microbrownian movement and this value of n_u° coincides with $n_u^\circ(\infty)$ as denoted by full vertical line in the figure. When some thermodynamic interactions between PET chains and water occur (in fact, the significant effects of water on the glass transition[8] and the melting[9] of PET were confirmed by DSC studies), $F'(n)$ for the wet PET fiber in the dyeing process may deviate from $F'(n)$ for the dry PET solid. Thus, $n_u^\circ(\infty)$ in Figure 9 does not always coincide with n_u° for infinite t_d at

given T_d estimated for the dry PET solid. Unfortunately, attempts to estimate $F'(n)$ for PET in water were not successful.

(2) Only the amorphous region belonging to the fraction between $n_u^\circ(t_2)$ and $n_u^\circ(t_1)$ is dyed during the dyeing time between t_2 and t_1.

(3) The dye uptake W by the amorphous region with $n_u < n_u^\circ(t_1)$ (*i.e.*, the region already dyed during t_1) is maintained constant during further dyeing ($t_d > t_1$).

(4) PET molecules in the amorphous region with higher n_u and those in the crystalline region are not dyed. The latter can be experimentally confirmed by the fact that the crystallinity, crystal size and crystal orientation of PET fibers evaluated by X-ray diffraction method do not change before and after dyeing.

In order to avoid confusion and misunderstanding, it should be noted that Figure 9(a)—(c) does not mean a one-dimensional diffusion of the dye from lower n_u to higher n_u. As described before, we defined the second-order structural elements as the aggregation of uniform polymeric chains, on the basis of segmental microbrownian movement. The second-order structural elements for a given polymer solid sample are separated from each other and arranged in the order of increasing n_u. The results indicate the $F'(n)$ value shown in Figure 2. Obviously, an increase in n_u° with t_d as a result of diffusion is expected to cause a rather three-dimensional nature of the dye molecules.

The amorphous regions having different n bring about a dramatic increase in the free volume fraction by occurrence of micro-Brownian movement above their T_g. The fractional free volume is generally given by

$$f = f_g + \Delta\alpha(T - T_g) \qquad (7)$$

where f_g is f ($\cong 0.025$) at T_g.

From eq 1′ and 7, n is obviously governed by the temperature T in a $\tan\delta$–T curve in α_a dispersion region and f is also closely related with T_g, as pointed out previously. Equation 7 means that the free volume fraction at temperature above T_g is larger for larger n.

Commercially available PET fibers have a degree of amorphous packing similar to sample code PD-5. The dye uptake of this sample, dyed at 130°C for 60 min, was 14.5 mg-dye/g-fiber for RBF, 16.5 mg-dye/g-fiber for DFO and 12.8 mg-dye/g-fiber for MFR, which correspond to $G(n_u^\circ)$ value of 0.21, 0.23, and 0.19, respectively. This means that when PET fibers having $G(n_u^\circ)$ larger than 0.21 at given T_d are dyed with RBF for 60 min, n_u° is a function of T_d and t_d (see Figure 6), and n_u° at $t_d = 60$ min can be determined experimentally with a given dye for a given T_d. The preparing conditions for the PET fiber samples with $G(n_u^\circ(100°C)) > 0.21$ were examined using variously prepared samples in our previous papers.[3,10,11] We found, for example, that the PET fibers spun with a spinning velocity ranging from 4.5 to 8.0 km min^{-1} and then annealed at a temperature T_a ranging from 250 to 255°C at a -5—$+5$% extension have never been dyed with RBF at 90°C. Then, in order to confirm the reliability of our theoretical prediction, these samples were dyed at 95°C with RBF and W was evaluated to be 12.3—13.6 mg-dye/g-fiber.

These results indicate that PET fibers are dyeable by commercially available disperse dyes even at 95°C, if the amorphous supermolecular structure of the fibers controlled in advance.

In conclusion, the parameter $G(n_u^\circ)$, defined in this article, can be regarded as an important structural factor governing the dyeability of PET fibers.

REFERENCES

1. K. Kitamura, F. Shibata, and Z. Yoshida, *Sen-i Gakkaishi*, **8**, 359 (1971).
2. K. Yonetake, T. Masuko, T. Shimanuki, and M. Karasawa, *J. Appl. Polym. Sci.*, **28**, 3049 (1983).
3. K. Kamide, T. Kuriki, and S. Manabe, *Polym. J.*, **18**, 167 (1986).
4. S. Manabe and K. Kamide, *Polym. J.*, **16**, 375 (1984).
5. S. Manabe, K. Kamide, C. Nakayama, and S.

Kobayashi, *J. Text. Mach. Soc. Jpn.*, **30**, T85 (1977), and also *J. Text. Mech. Soc. Jpn., English Edition*, **27**, 10 (1981).
6. C. Nakayama, K. Kamide, and S. Manabe, *Sen-i Gakkaishi*, **33**, T-192 (1977).
7. K. Kamide, T. Kuriki, and S. Manabe, *Polym. J.*, **18**, 163 (1986).
8. T. Hatakeyama and H. Hatakeyama, *Sen-i Gakkaishi*, **39**, T461 (1983).
9. K. Kamide, T. Kuriki, and M. Saito, unpublished results.
10. T. Kuriki, S. Manabe, and K. Kamide, *J. Text. Mach. Soc. Jpn.*, **38**, T150 (1985).
11. T. Kuriki, K. Kamide, and Y. Komatsu, *J. Text. Mach. Soc. Jpn.*, **38**, T192 (1985).